The influence of gas phase reactions on the design criteria for catalysts for lean NO$_x$ reduction with dimethyl ether

Stefanie Tamm [a,b,*], Hanna H. Ingelsten [a,b], Magnus Skoglundh [a,b], Anders E.C. Palmqvist [a,b]

[a] Competence Centre for Catalysis, Chalmers University of Technology, SE-412 96 Göteborg, Sweden
[b] Applied Surface Chemistry, Chalmers University of Technology, SE-412 96 Göteborg, Sweden

ARTICLE INFO

ABSTRACT

In the selective catalytic reduction (SCR) of NO by dimethyl ether (DME), the formation of unexpectedly high amounts of NO$_2$ over 300 °C has previously been reported. In this study, we explain this phenomenon by radical reactions initiated by DME and O$_2$, during which DME is partly oxidized and NO$_2$ is formed in the presence of NO. For the design criteria of a DME-SCR catalyst, these gas phase reactions have mainly three consequences: (i) another type of reducing agent than that fed into the reactor reaches the catalyst, (ii) no activation of the reducing agent such as partial oxidation is required, and (iii) several of the proposed intermediate species for HC-SCR, e.g. NO$_2$, HONO, CH$_3$–NO$_2$, and CH$_3$–NO form already in the gas phase. An efficient DME-SCR catalyst should thus have high selectivity for reduction of NO$_x$ predominately by partially oxidized C$_1$-compounds, and it should not have particularly strong oxidizing properties to avoid non-selective oxidation of these C$_1$-compounds. These two requirements appear to be reasonable well met by the acidic zeolite H-ZSM-5.

1. Introduction

The interest in research and investments in alternative fuels has increased over the last years due to the concern for global climate change caused by increasing atmospheric CO$_2$ concentrations and the limited fossil fuel resources available to support the growing energy demand. One of the most energy effective and low CO$_2$ emitting alternative fuels is dimethyl ether (DME) produced from biomass gasification [1,2]. As fuel for internal combustion engines, DME has the advantages of a high cetane number and producing very low amounts of soot during its combustion in the diesel process [3–5]. However, vehicles with DME-fuelled combustion engines will most likely need after-treatment technologies to further reduce NO$_x$ emissions to meet the most stringent upcoming legislations.

In dry exhaust gases, Co/Al$_2$O$_3$, MoO$_3$/Al$_2$O$_3$ and pure γ-Al$_2$O$_3$ catalysts were reported active for selective catalytic reduction of NO$_x$ (DME-SCR) [6,7]. In contrast, it was found that the two currently most promising HC-SCR catalysts for after-treatment of diesel-exhaust, namely Ag/Al$_2$O$_3$ and Cu-ZSM-5 are not particularly active for the DME-SCR in the presence of water [8,9].

However, the acidic form of zeolite ZSM-5 (H-ZSM-5) has recently shown to be a promising catalyst for DME-SCR also in the presence of water [10]. During the evaluation of H-ZSM-5 as DME-SCR catalyst, unexpectedly high amounts of NO$_2$ were observed above 300 °C. This formation of NO$_2$ depended on the DME concentration and was proposed to be related to gas phase reactions in the presence of DME and NO. In the present study, we investigate these gas phase reactions in more detail and evaluate the role of the catalyst during DME-SCR.

2. Experimental methods

2.1. Catalyst preparation

Zeolite H-ZSM-5 powder (batch number: 2125120, Akzo Nobel Catalysts BV) with a SiO$_2$/Al$_2$O$_3$ molar ratio of 40 was used as received. More detailed properties of the H-ZSM-5 powder have been published elsewhere [11]. For catalytic activity experiments in a flow reactor, a cylindrical honeycomb structured cordierite monolith (400 cpsi, 2 cm long, and 2 cm in diameter) was coated with the zeolite powder. For the washcoating procedure, catalyst powder and silica binder (Bindzil colloidal silica 30NH$_3$/200, Eka Chemicals) were mixed with Milli-Q water to obtain a slurry. The weight ratio of the catalyst powder and the silica was 4:1. The monolith was immersed in the slurry, and excess liquid was removed by gently blowing air through the channels and on the outside of the monolith sample. Subsequently, the sample was

* Corresponding author at: Applied Surface Chemistry and Competence Centre for Catalysis, Department of Chemical and Biological Engineering, Chalmers University of Technology, SE-412 96 Göteborg, Sweden, Tel.: +46 0 31 772 2977, fax: +46 0 31 16 00 62.
E-mail address: stamm@chalmers.se (S. Tamm).

dried in air at 90 °C and calcined at 600 °C for 2 min. This procedure was repeated until the washcoat represented 20 wt% of the total sample weight. Finally, the sample was calcined in air for 2 h at 550 °C. The specific surface area was measured to 60 m^2/g_{sample} according to the BET method. This surface area corresponds to 355 m^2/g for the zeolite powder.

2.2. Activity tests

In order to evaluate the effect of the gas phase reactions and establish design criteria for a catalyst for DME-SCR, experiments were carried out both with and without the catalyst in the reactor. A horizontally mounted quartz-tube reactor was used for all the flow-reactor experiments. In the activity tests with the catalyst, the temperature was controlled in the gas stream before the catalyst and was also measured inside a channel in the centre of the monolith. In the gas phase experiments (without the catalyst), the thermocouple, which controls the gas temperature, was situated at the same place as in the experiments with the catalyst. The feed gases were mixed by a computerized multi component gas mixer (Environics 2000) and water was introduced to the system via a separate oven. The reactor exhaust gas composition was analyzed by a gas phase FTIR instrument (mks-instruments, MultiGas 2030) with the gas cell heated to 191 °C.

Gas phase experiments were carried out as temperature ramps. The empty reactor was heated to 200 °C in an Ar flow of 3500 ml/min, corresponding to a residence time of the gas mixture inside the reactor of approximately 6 s at room temperature. After heating the reactor, a background spectrum was collected at 200 °C and, in the experiments with additional water, the water was subsequently introduced. This water flow was allowed to stabilize for 15 min before the feed gas composition was changed to contain DME, NO_x, O_2 and water, and left to stabilize for additional 5 min before the temperature ramp was started. The reactor was heated at a rate of 10 °C/min to 550 °C, where it was held for 5 min for stabilization and cooled at 10 °C/min to 200 °C. Two temperature ramps (heating and cooling) were performed for each gas mixture. Oxidation of DME was carried out with either 250 or 1000 ppm DME and 8% O_2. Furthermore, temperature ramps were performed with a gas mixture of 8% O_2, 500 ppm NO_x (NO or NO_2), and 250, 500, 1000 or 2000 ppm DME either in the presence of 5% water or without water and balanced with Ar. Both NO and NO_2 were evaluated as NO_x source.

In contrast to the gas phase experiments, the activity tests with the catalyst were carried out as steady state experiments. Before each experiment, the catalyst was pre-treated in a gas stream of 8% O_2 in Ar at 550 °C for 30 min. Catalytic activity tests were performed with 5% water in a feed gas mixture of 7.6% O_2, 475 ppm NO_x, and 475, 950 or 1900 ppm DME and balanced with Ar. Starting at 500 °C with a DME/NO_x ratio of 1, the DME inlet concentration was stepwise increased, dwelling 15 min at each step. After the step with the highest DME concentration, the catalyst was cooled in Ar to the next reaction temperature, and the procedure was repeated. All the activity experiments and the pre-treatment were performed with a total flow of 3500 ml/min, corresponding to a space velocity of 33,400 h^{-1}.

For the evaluation, the conversion of NO_x is defined as $(1 − [NO_{x,out}]/[NO_{x,in}]) \times 100\%$ and the conversion of DME as $(1 − [DME_{out}]/[DME_{in}]) \times 100\%$. The yield of CO, CO_2, formaldehyde, formic acid, and methanol is defined as $[gas_{out}]/2[DME_{in}] \times 100\%$, and the yield of nitric acid is defined as $[HNO_{3,out}]/[NO_{x,in}] \times 100\%$. The gas phase FTIR instrument, used to monitor the gas composition, calculates the concentrations of different gases according to calibration curves using N_2 as carrier gas. For the reported experiments, however, Ar has been used as carrier gas. Differences in measured concentrations that depend on the carrier gas are less

than 10%. Reported concentrations have not been compensated for the differences except for NO, NO_2 and NO_x.

3. Results and discussion

3.1. Gas phase reactions

In this study, it is shown that gas phase reactions occurring before the catalyst under conditions for DME-SCR considerably change the feed gas composition reaching the catalyst. Gas phase reactions between DME and oxygen have previously been reported in the context of pyrolysis of DME [12]; from a combustion and ignition point of view in engines [13,14]; or in simulated degradation of DME in the atmosphere [15]. In these studies the pressure was typically between 1 and 10 bar and the oxygen concentration was 0.2 to 2 times the value of the stoichiometric value for complete oxidation. In the present communication, the oxidation of DME was studied in excess O_2 in a flow reactor under atmospheric pressure. The conversion of DME and the formation of CO and formic acid reach a maximum between 300 and 350 °C as shown in Fig. 1. The formation of formaldehyde increases with temperature and only minor amounts of CO_2 are observed between 200 and 550 °C. This is in accordance with Liu et al. [13], who conducted similar flow reactor experiments. The conversion of DME and the yields of the above mentioned compounds do not depend on the absolute DME concentration for the two concentrations studied. Furthermore, the concentrations are similar during heating and cooling ramps. The observed gas compositions at certain temperatures can be explained by well-established and published chemical models for the oxidation of DME, which are based on radical reactions, typical for low-temperature ignition of hydrocarbons [12,14,16,17]. According to these published models, the conversion of DME is initiated in the flow reactor by reaction
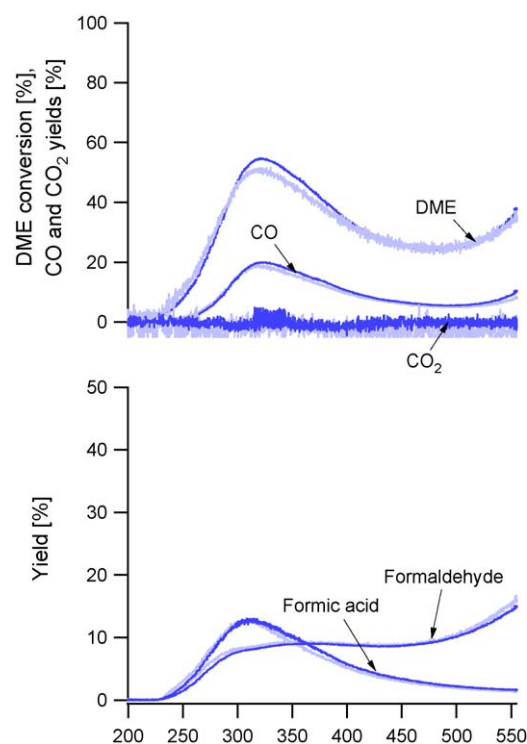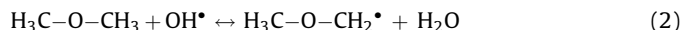

Fig. 1. DME oxidation as function of temperature with two different DME concentrations, in a gas mixture of 8% O_2 and 250 ppm DME (light blue) or 1000 ppm DME (dark blue) balanced in Ar. Both heating and cooling ramps are included (For interpretation of the references to color in this figure legend, the reader is referred to the web version of the article).

(1) where DME splits into an $H_3CO^\bullet$ radical and a $CH_3^\bullet$ radical.

$$H_3C-O-CH_3 \leftrightarrow H_3CO^\bullet + CH_3^\bullet \qquad (1)$$

In a following published scheme of complex radical reactions, $OH^\bullet$ radicals are formed, which in turn initiate the oxidation of other DME molecules by abstraction of a hydrogen atom giving a methoxymethyl radical ($H_3C-O-CH_2^\bullet$) according to reaction (2) [16,18,19].

$$H_3C-O-CH_3 + OH^\bullet \leftrightarrow H_3C-O-CH_2^\bullet + H_2O \qquad (2)$$

These methoxymethyl radicals have been shown to react with O_2 giving the peroxy radical $H_3C-O-CH_2OO^\bullet$ (reaction (3)), which
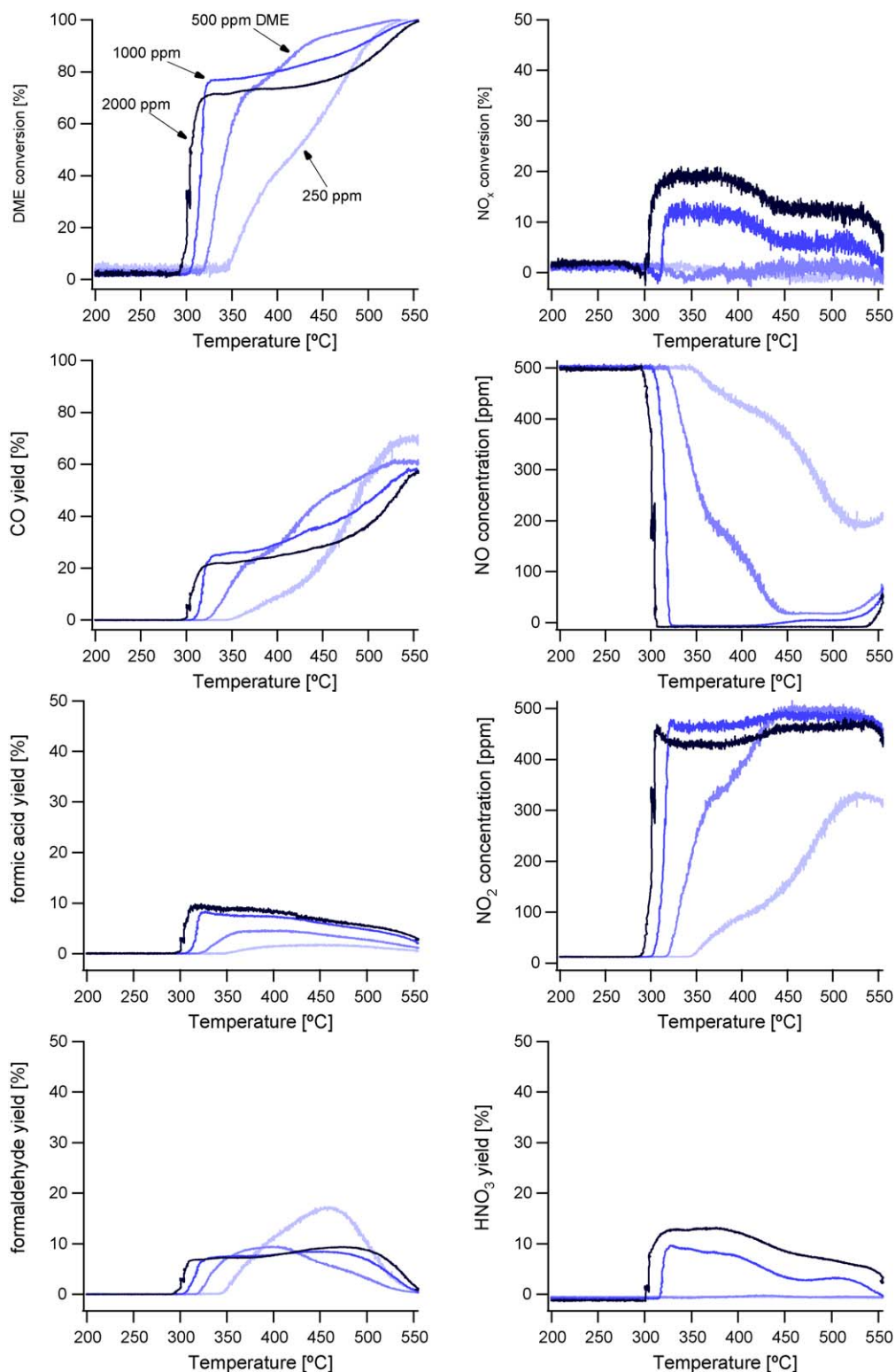

Fig. 2. Gas phase reactions with DME, NO and O_2 as function of temperature with different DME concentrations, in a gas mixture of 500 ppm NO, 8% O_2 and 250 ppm DME (light blue), 500 ppm DME (darker blue), 1000 ppm DME (dark blue) or 2000 ppm DME (black) balanced in Ar. Both heating and cooling ramps are included (For interpretation of the references to color in this figure legend, the reader is referred to the web version of the article).

has been proposed to be a key intermediate in the oxidation of DME [17].

$$H_3C-O-CH_2^\bullet + O_2 \leftrightarrow H_3C-O-CH_2OO^\bullet \tag{3}$$
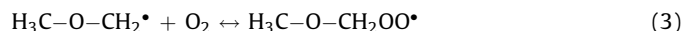
The peroxy radicals (formed by reaction (3)) have found to readily isomerize to $CH_2-O-CH_2OOH^\bullet$, which thermally decomposed via a chain propagation step to two formaldehyde molecules and one $OH^\bullet$ radical (reaction (4)) [19].

$$CH_2-O-CH_2OOH^\bullet \rightarrow 2HCHO + OH^\bullet \tag{4}$$
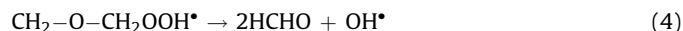
Alternatively, as a chain branching reaction, the peroxy radicals were reported to react further with O_2 and decompose in a sequence of steps into two $OH^\bullet$ radicals, one formaldehyde molecule and one $HCOO^\bullet$ radical (reaction (5)) [19].

$$CH_2-O-CH_2OOH^\bullet + O_2 \rightarrow 2OH^\bullet + HCHO + HCOO^\bullet \tag{5}$$
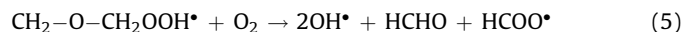
The $HCOO^\bullet$ radicals were proposed to react with DME and form formic acid [19]. The formation of higher amounts of formic acid than of formaldehyde, as observed in our experiments in the temperature range between 250 and 350 °C in Fig. 1, cannot be explained by the stoichiometry of reactions (4) and (5). However, reactions between formaldehyde molecules and $OH^\bullet$ radicals (reaction (6)) and between formaldehyde molecules and $HCOO^\bullet$ radicals (reaction (7)) as included in the reaction scheme by Dagaut et al. [19] allow for a wider range of formaldehyde to formic acid ratios.

$$HCHO + OH^\bullet \leftrightarrow HCOOH + H^\bullet \tag{6}$$

$$HCHO + HCOO^\bullet \leftrightarrow HCOOH + CHO^\bullet \tag{7}$$

Above 325 °C, an increase in temperature leads to a decrease in the oxidation of DME as shown in Fig. 1. This phenomenon is qualitatively in accordance with published findings [13,14] and has been explained by a decrease in the ratio of the chain branching reaction (reaction (5)) to the chain propagation reaction (reaction (4)) with increasing temperature.

Adding NO to the gas mixture of DME and O_2, dramatically changes the oxidation of DME with temperature, as shown in Fig. 2. No reaction is observed below 300 °C for any of the DME concentrations. Above this temperature and for DME/NO ratios of 2 and 4, the conversion of DME sharply increases to over 70% conversion in a temperature interval of less than 20 °C. At lower DME/NO ratios, the increase in the conversion of DME is shifted to higher temperatures and is less sharp. No decrease in conversion with increasing temperature is observed in any of these experiments. At the temperature, where oxidation of DME starts, large amounts of NO_2 are formed and the concentration of NO decreases considerably. The results further reveal the conversion of some NO_x in the same temperature interval where nitric acid is formed. Unfortunately, we cannot quantify the amount of formed nitric acid due to deposition of nitric acid on the windows of the gas phase FTIR instrument perturbing the quantification. However, it is reasonable to assume that the observed conversion of NO_x is equivalent to the formation of nitric acid, since the shape of the conversion of NO_x and the formation of nitric acid perfectly mimic each other.

In Fig. 2, it is further shown that the oxidation of DME is sensitive to the DME/NO ratio. The conversion of DME, the oxidation of NO, and the yields of CO, formic acid, formaldehyde, and nitric acid are shifted to lower temperatures with increasing DME/NO ratios up to a DME/NO ratio of 2 and are approximately stable at higher DME/NO ratios. The conversion of DME and the yield of formic acid increase with increasing DME/NO ratio, while the yield of formaldehyde decreases.

Comparing experiments with and without NO in the feed (Figs. 2 and 1, respectively), it can be seen that addition of NO to the gas mixture inhibits the oxidation of DME and the formation of CO below 300 °C, and enhances these reactions above 400 °C. Formation of formic acid starts at higher temperatures and the yields are lower in the presence of NO. Decreasing the DME/NO ratio enlarges the temperature window where the oxidation of DME is inhibited. Furthermore, the yield of formic acid decreases, and the yield of formaldehyde increases. The main observations of inhibited oxidation of DME and the formation of NO_2 upon addition of NO are in accordance with the findings reported by Liu et al. and Dagaut et al. [13,19].

Addition of an additional gas to a mixture of DME and O_2 increases the number of possible reactions and intermediates. Especially, since $NO^\bullet$ and $NO_2^\bullet$ need here to be considered as radicals, according to the IUPAC definition that radicals are atoms or groups of atoms with one or more unpaired electrons [20]. Dagaut et al. [19], who modelled the oxidation of DME in the
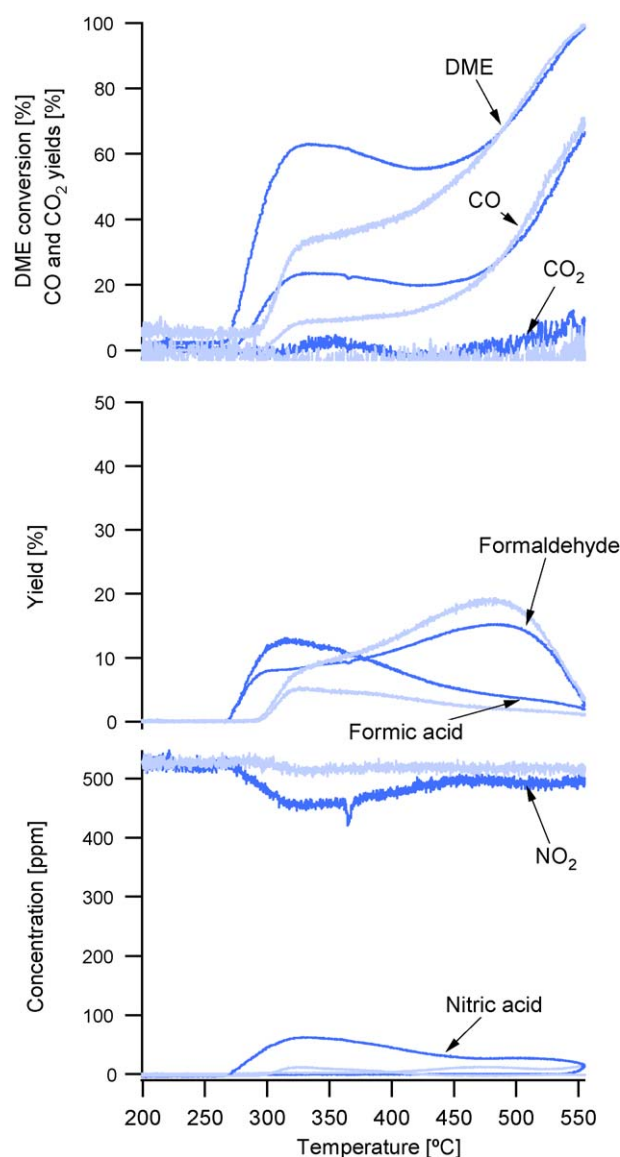

Fig. 3. Gas phase reactions with DME, NO_2 and O_2 as function of temperature with two different DME concentrations, in a gas mixture of 500 ppm NO_2, 8% O_2 and 250 ppm DME (light blue) or 1000 ppm DME (dark blue) balanced in Ar. Both heating and cooling ramps are included (For interpretation of the references to color in this figure legend, the reader is referred to the web version of the article).

presence of NO and O_2, found that the chain branching reaction (5) becomes less important because the methoxymethyl peroxy radical ($H_3C-O-CH_2OO^\bullet$), formed by reaction (3), also reacts with NO forming NO_2 (reaction (8)).

$$H_3C-O-CH_2OO^\bullet + NO^\bullet \leftrightarrow CH_3OCH_2O^\bullet + NO_2^\bullet \qquad (8)$$
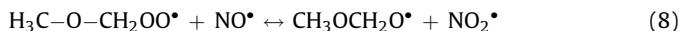
They suggest that this is the reason for the observed inhibited oxidation of DME below 300 °C. However, the formation of the methoxymethyl peroxy radical indicates, that a chain of radical reactions has occurred, since this radical is not one of the radicals which are formed from the initial dissociation of DME. It appears thus less likely, that reaction (8) is the main reason for the inhibited oxidation below 300 °C, since no NO_2 was detected at this temperature. Moreover, it seems not likely, that a chain of radical reactions can take place without any observable DME conversion. Termination reactions between $CH_3^\bullet$ and $OCH_3^\bullet$ radicals, which are formed from the initial dissociation of DME, and $NO^\bullet$ radicals (reactions (9) and (10)) are probably more efficient in shifting the onset of the DME oxidation to higher temperatures. The amount of the products of these termination reactions may be so small that we cannot detect them with our analysis instruments.

$$CH_3^\bullet + NO^\bullet \leftrightarrow CH_3-NO \qquad (9)$$

$$OCH_3^\bullet + NO^\bullet \leftrightarrow H_2CO + HNO \qquad (10)$$

According to the same researchers [19], $HOO^\bullet$ radicals are formed in a complex scheme of radical reactions and the reaction between $NO^\bullet$ and these $HOO^\bullet$ radicals (reaction (11)) becomes an important source for $OH^\bullet$ radicals above about 300 °C. This would explain the dramatic increase of the oxidation of DME at this temperature.

$$HOO^\bullet + NO^\bullet \leftrightarrow OH^\bullet + NO_2^\bullet \qquad (11)$$

Reactions between NO and other radicals (reactions (8) and (11)) affect the number of $OH^\bullet$ radicals and thus provide an explanation to the effect of the DME/NO ratio on the overall DME oxidation. At high DME/NO ratios, the possibility of forming $HOO^\bullet$ from DME or a partially oxidized compound, and hereby accelerating the oxidation of DME, is higher than at low DME/NO ratios, which is in accordance with the results presented in Fig. 2. In contrast, the probability to inhibit the overall oxidation of DME by reactions (8)–(10) is higher at low DME/NO ratios.

The observed formation of nitric acid (Fig. 2) cannot be explained by the previously published model by Dagaut et al. [19]. However, nitrous acid (HONO) and hyponitrous acid (HNO) are part of the model, and HONO is predicted to accumulate below 350 °C in a gas mixture of 4000 ppm DME, 24,000 ppm O_2 and 500 ppm NO [19]. In the atmosphere of the earth, it is known that nitrous acid is oxidized to nitric acid in aerosols or small water droplets [21]; and in the context of NH_3-SCR, HONO is regarded as
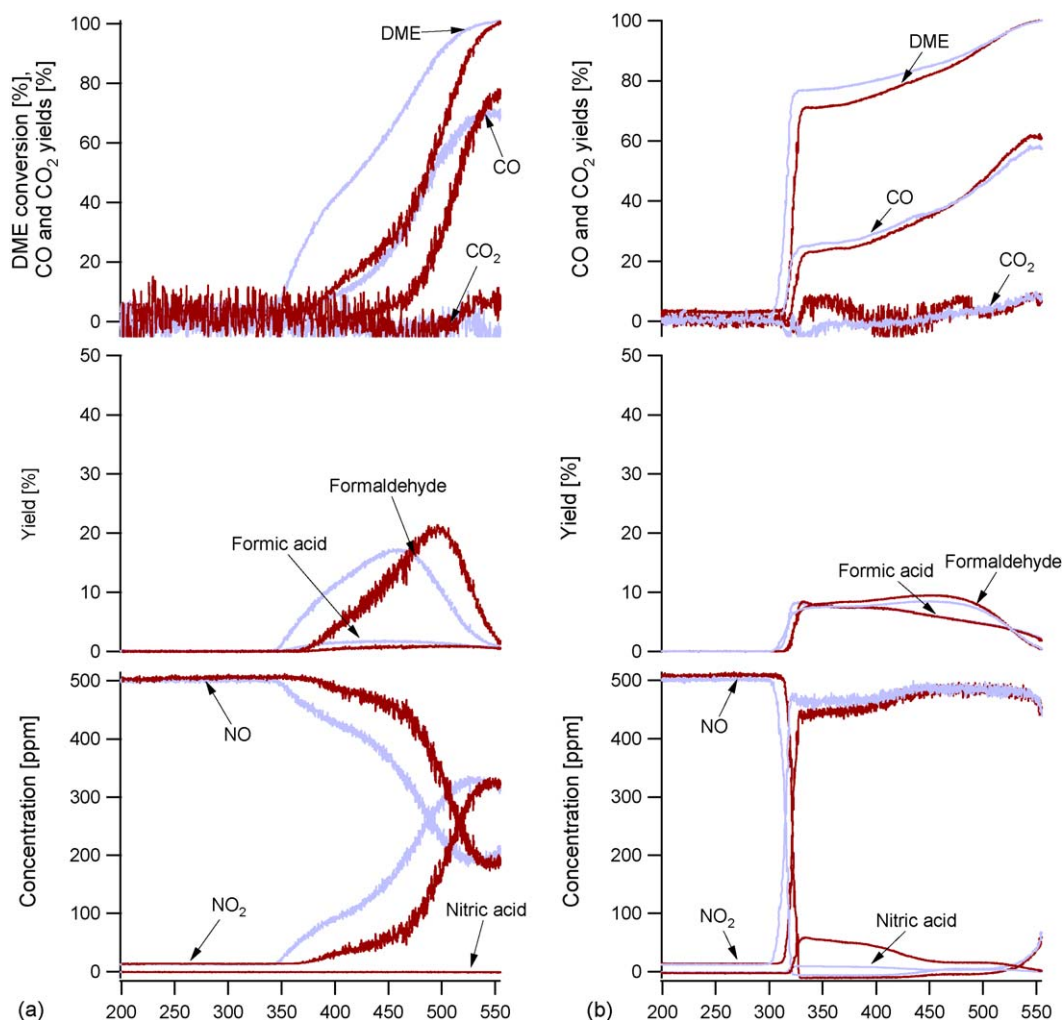

Fig. 4. Gas phase reactions with DME, NO and O_2 as function of temperature without water (light blue) and with 5% water (dark red) with two different DME concentrations, in a gas mixture of 500 ppm NO, 8% O_2 and (a) 250 ppm DME or (b) 1000 ppm DME balanced in Ar. Both heating and cooling ramps are included (For interpretation of the references to color in this figure legend, the reader is referred to the web version of the article).

very reactive [22]. The observed nitric acid is thus likely formed by oxidation of nitrous acid. These conclusions are consistent with the observation, that no reaction was observed between 200 and 550 °C in a gas mixture of only DME and NO (results not shown).

Fig. 3 shows the results of an experiment with DME, O_2 and NO_2 in the feed gas mixture. Oxidation of dimethyl ether starts at about 270 °C, and CO, formaldehyde and formic acid are formed. For a DME/NO_2 ratio of 2, some NO_2 is converted and nitric acid is formed (not shown). Comparing the results in the presence and absence of NO_2, shows that NO_2 inhibits the oxidation of DME below about 450 °C and promotes its oxidation above this temperature. The degree of inhibition is dependent on the DME/NO_2 ratio. However, these effects are much less pronounced in the presence of NO_2 than in the presence of NO. Analogous to the reactions with NO, the inhibition of DME oxidation can be explained by a termination reaction between NO_2 and a radical as in reaction (12).

$$CH_3^\bullet + NO_2^\bullet \leftrightarrow CH_3-NO_2 \qquad (12)$$

Dagaut et al. [19] proposed reactions between NO_2 and DME or partly oxidized DME as $H_3CO^\bullet$ yielding HONO (reaction (13) and (14)).

$$H_3C-O-CH_3 + NO_2^\bullet \leftrightarrow H_3C-O-CH_2^\bullet + HONO \qquad (13)$$

$$H_3CO^\bullet + NO_2^\bullet \leftrightarrow H_2CO + HONO \qquad (14)$$
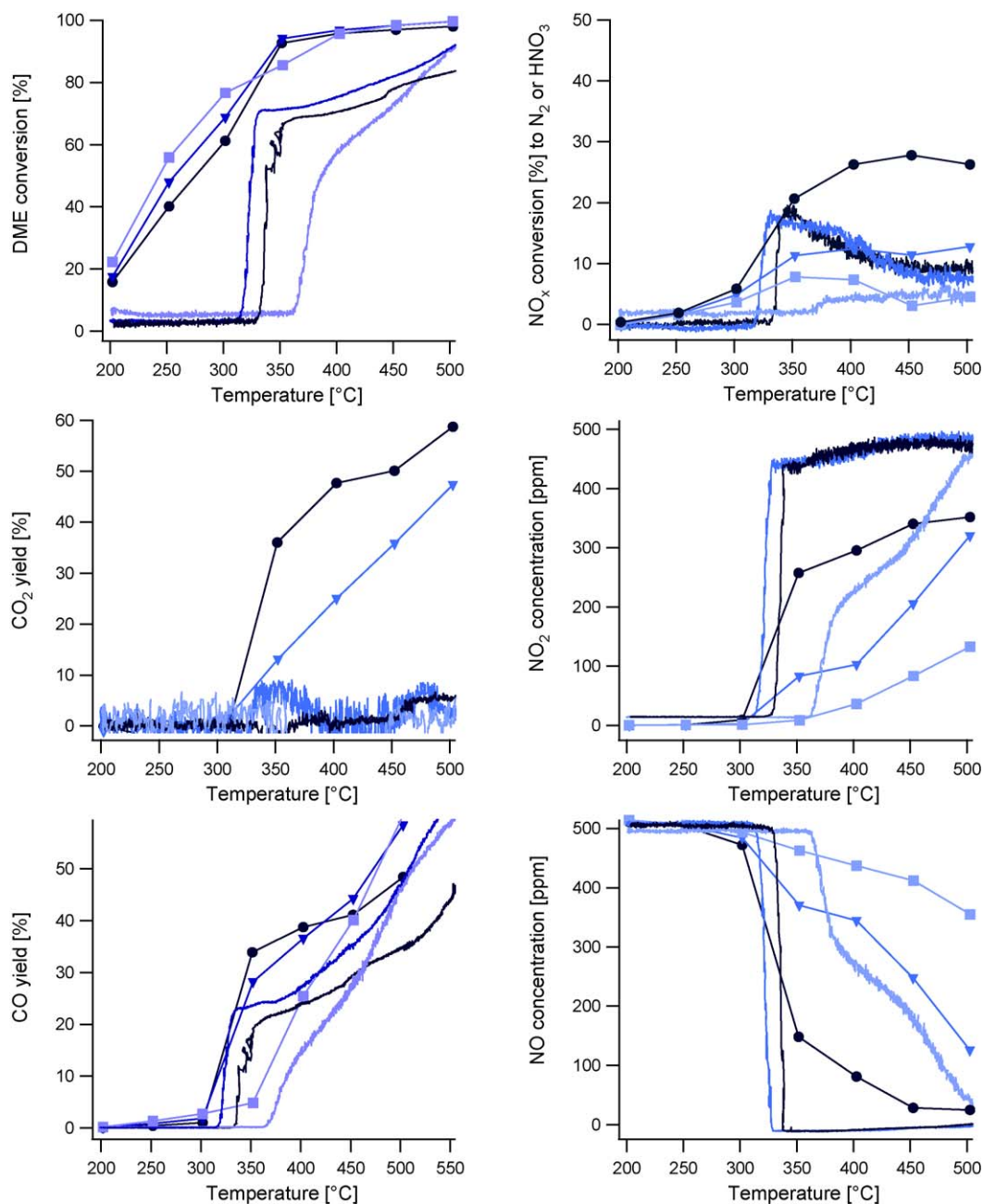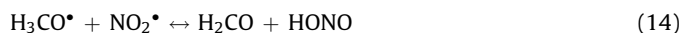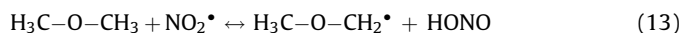

Fig. 5. Comparison of gas composition between gas phase reactions (full line, heating ramp) and an H–ZSM-5 catalyst (symbols, steady state experiments) with DME, NO, O_2 and 5% water as function of temperature with different DME concentrations, in a gas mixture of 500 ppm NO, 8% O_2 and 500 ppm DME (light blue, ■), 1000 ppm DME (dark blue, ▼) or 2000 ppm DME (black, ●) balanced in Ar. NO_x conversion with catalyst shows high selectivity to N_2, whereas without catalyst the selectivity is high to HNO_3 (For interpretation of the references to color in this figure legend, the reader is referred to the web version of the article).

These reactions are the likely source of the observed nitric acid in our experiments and reaction (13) explains the promotion of the oxidation of DME at higher temperatures.

Addition of water to a gas mixture of DME, NO and O_2 further changes the gas composition. In Fig. 4a and b the gas compositions of similar experiments with two different DME/NO ratios with and without water are shown as a function of temperature. In the presence of water, the oxidation of DME, and the formation of CO and NO_2 start at higher temperatures than without water, for both DME/NO ratios studied. The formation of formaldehyde increases and the formation of formic acid decreases. At a DME/NO ratio of 2, the formation of nitric acid increases in the presence of water.

Adding water to the feed gas mixture of DME, NO and O_2 has similar consequences as decreasing the DME/NO_x ratio as seen by comparing Figs. 2 and 4. In the latter context, the degree of DME oxidation has previously been explained by the number of OH$^\bullet$ radicals available for the reaction. In general, it is not expected that addition of water would decrease the number of OH$^\bullet$ radicals. However, the presence of 5% water shifts the equilibrium of reaction (2) to the left, leading to lower consumption of OH$^\bullet$ radicals. This shift decelerates the overall DME oxidation rate. In parallel, formation of higher amounts of nitric acid is observed in the presence of water, and the reaction between NO_2 and water is one possible source for nitric acid in the experiment. In the presence of O_2, however, the equilibrium of this reaction does not favour nitric acid formation at temperatures above 200 °C. It is thus more likely, that introduction of water changes the ratio of the radical reactions in favour of reactions forming nitric, nitrous or hyponitrous acid. However, the importance of these reactions for the whole process can only be revealed by a detailed model.

3.2. Influence of the H-ZSM-5 catalyst

During conditions for DME-SCR the discussed gas phase reactions will occur in the reactor tube before the gases reach the catalyst. The influence of the catalyst on the reaction is thus the difference between the gas compositions leaving the empty reactor and the reactor containing the catalyst as shown in Fig. 5. The main effect of the H-ZSM-5 catalyst is the reduction of NO_x to N_2 (formation of N_2 is not shown) with a maximum of 28% NO_x reduction at 450 °C at a DME/NO_x ratio of 4. Furthermore, in a gas stream of DME, O_2, NO and water the catalyst increases the conversion of DME and the formation of methanol (not shown), especially below 300 °C. Above 300 °C, the catalyst increases the formation of CO_2 and formaldehyde and the conversion of NO_x, but lowers the concentration of NO_2. Only negligible amounts of nitric acid and formic acid are observed in the presence of the H-ZSM-5 catalyst (not shown), in contrast to the experiments with the empty reactor (Fig. 2). The catalyst has only a minor effect on the formation of CO as shown in Fig. 5.

The major part of the increase in the conversion of DME below 300 °C in presence of the catalyst is due to hydrolysis of DME to methanol (reaction (15)).

$$H_3C\!-\!O\!-\!CH_3 + H_2O \leftrightarrow 2H_3COH \qquad (15)$$

The equilibrium for this reaction favours the formation of methanol above 200 °C with less than stoichiometric amounts of water. With increasing concentrations of water, methanol formation is favoured at even lower temperatures. Although the concentration of water on the catalyst surface is not known, we can assume that the equilibrium of reaction (15) is in favour of the formation of methanol, explaining the formation of methanol below 350 °C. Above 350 °C, the major part of the DME has already reacted in the gas phase reactions, before it reaches the catalyst and is, thus, no longer available for the formation of methanol. This
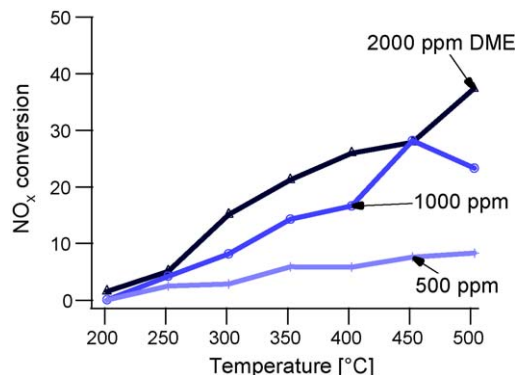

Fig. 6. NO_x conversion over a H-ZSM-5 catalyst with DME, NO_2, O_2 and 5% water as function of temperature with different DME concentrations, in a gas mixture of 500 ppm NO, 8% O_2 and 500 ppm DME (light blue, +), 1000 ppm DME (dark blue, ○) or 2000 ppm DME (black, △) balanced in Ar (For interpretation of the references to color in this figure legend, the reader is referred to the web version of the article).

can explain the smaller difference in DME conversion in the experiments with and without catalyst above 350 °C. When using NO_2 as the NO_x source, the maximum conversion of NO_x is 37%, which is reached at 500 °C and a DME/NO_x ratio of 4 as shown in Fig. 6. The conversion of NO_x is in general higher with NO_2 in the feed than with NO. In a previous study [10], we speculated that this phenomenon could be explained if more DME is available on the catalyst in the presence of NO_2 due to less gas phase reactions. The results presented in Fig. 3 support this statement. Reduction of NO_x, formation of NO and CO_2, and the conversion of nitric acid and formic acid are thus the main processes that occur on the H-ZSM-5 catalyst, at temperatures where gas phase reactions take place.

It has been shown that oxidation of NO to NO_2 is an important step for NO reduction over many zeolite based catalysts [23–26]. Furthermore, Cant et al. [23] suggested that adsorbed NO_2 is involved in the initial C–H bond breaking and formation of HONO in methane-SCR over a Co-ZSM-5 catalyst. The formed methyl radical can react further with either NO or NO_2 to nitrosomethane (CH_3–NO) or nitromethane (CH_3–NO_2) [23], respectively. Nitromethane and nitrosomethane have also been proposed by several authors to be intermediates which decompose via HNCO or HCN to NH_3 [23,27,28]. Ammonia, in turn is known from NH_3-SCR to efficiently reduce NO_x to N_2. Yeom et al. [22,29] propose in more detail that HONO reacts with ammonia to ammonium nitrite, which subsequently decomposes to N_2 and water over zeolite and Al_2O_3-based catalysts. Comparing the proposed reactions and intermediates over zeolite based catalysts with the reactions and species discussed in this paper, it is apparent that several compounds (NO_2, nitrous acid (HONO), nitromethane (CH_3–NO_2) and nitrosomethane (CH_3–NO)) which are considered as intermediates in NO_x reduction in HC-SCR are already formed in the gas phase in DME-SCR. In contrast to a HC-SCR catalyst for non-oxygenated hydrocarbons, a DME-SCR catalyst needs only to promote the reactions from nitromethane or nitrosomethane to N_2 but should not catalyze the oxidation of the already formed intermediates by molecular oxygen.

4. Conclusions

Gas phase reactions between DME, oxygen, NO_x and water considerably affect the composition of the feed gas reaching the DME-SCR catalyst. In mixtures containing DME and oxygen, oxidation of DME occurs via complex radical reactions, where the methoxymethyl peroxy radical (H_3C–O–$CH_2OO^\bullet$) plays a central role. In the presence of NO, DME and O_2, the oxidation of DME is promoted at higher temperatures and inhibited below

300 °C probably by a termination reaction involving $NO^\bullet$ and the DME-derived radicals. Introduction of water to the system further widens the temperature window of inhibition of the oxidation of DME at lower temperatures and promotes DME-oxidation at higher temperatures.

Since several of the proposed intermediate species for HC-SCR such as NO_2, HONO, CH_3–NO_2, and CH_3–NO are already formed in the gas phase the role of a DME-SCR catalyst differs considerably compared to conventional HC-SCR catalysts for non-oxygenated hydrocarbons. An efficient DME-SCR catalyst should thus have high capability to reduce NO_x using partially oxidized C_1-compounds, does not need to be able to activate the reducing agent and should not unselectively oxidize the species previously formed in the gas phase reactions. Compared to Ag-ZSM-5, Ag/Na-ZSM-5 and Cu-ZSM-5, which have been reported not to be suitable for DME-SCR [8,10], the acidic zeolite H-ZSM-5 meets these criteria comparably well.

Acknowledgements

References

[1] P. Ahlvik, Å. Brandberg, Well-to-wheel efficiency for alternative fuels from natural gas and biomass,, 1st ed., Swedish National Road Administration, Borlänge, 2001, pp. 1–121, http://www.vv.se/filer/publikationer/2001-85.pdf (2007-10-11).

[2] R. Edwards, J.-F. Larivé, V. Mahieu, R. Rouveirolles, Well-to-wheels analysis of future automotive fuels and powertrains in the European context (2006) http://www.co2star.eu/publications/Well_to_Tank_Report_EU.pdf (2009-02-10).

[3] T.A. Semelsberger, R.L. Borup, H.L. Greene, J. Power Sources 156 (2006) 497–511.

[4] T. Fleisch, C. McCarthy, A. Basu, C. Udovich, P. Charbonneau, W. Slodowske, S.-E. Mikkelsen, J. McCandless, in: Proceedings of the SAE International Congress and Exposition, Detroit, Michigan, USA, 1995.

[5] S.C. Sorenson, S.-E. Mikkelsen, in: Proceedings of the SAE International Congress and Exposition, Detroit, Michigan, USA, 1995.

[6] M. Alam, O. Fujita, K. Ito, Proc. Inst. Mech. Eng. Part A: J. Power Energy 218 (2004) 89–95.

[7] S.G. Masters, D. Chadwick, Appl. Catal. B 23 (1999) 235–246.

[8] S. Erkfeldt, A.E.C. Palmqvist, E. Jobson, Top. Catal. 42–43 (2007) 149–152.

[9] K. Masuda, K. Tsujimura, K. Shinoda, T. Kato, Appl. Catal. B 8 (1996) 33–40.

[10] S. Tamm, H.H. Ingelsten, A. Palmqvist, Catal. Lett. 123 (2008) 233–238.

[11] H.H. Ingelsten, D.M. Zhao, A. Palmqvist, M. Skoglundh, J. Catal. 232 (2005) 68–79.

[12] Z. Zhao, M. Chaos, A. Kazakov, F.L. Dryer, Int. J. Chem. Kinet. 40 (2008) 1–18.

[13] I. Liu, N.W. Cant, J.H. Bromly, F.J. Barnes, P.F. Nelson, B.S. Haynes, Chemosphere 42 (2001) 583–589.

[14] P. Dagaut, C. Daly, J. Simmie, M. Cathonnet, in: Proceedings of the 27th Symposium (International) on Combustion, The Combustion Institute, 1998 , pp. 361–369.

[15] S. Langer, E. Ljungstrom, T. Ellermann, O.J. Nielsen, J. Sehested, Chem. Phys. Lett. 240 (1995) 53–56.

[16] A. Andersen, E.A. Carter, J. Phys. Chem. A 107 (2003) 9463–9478.

[17] J. Sehested, T. Møgelberg, T.J. Wallington, E.W. Kaiser, O.J. Nielsen, J. Phys. Chem. 100 (1996) 17218–17225.

[18] C.M. Rosado-Reyes, J.S. Francisco, J.J. Szente, M.M. Maricq, L.F. Ostergaard, J. Phys. Chem. A 109 (2005) 10940–10953.

[19] P. Dagaut, J. Luche, M. Cathonnet, Combust. Sci. Technol. 165 (2001) 61–84.

[20] W.H. Koppenol, Pure Appl. Chem. 72 (2000) 437–446.

[21] P.K. Mudgala, S.P. Bansala, K.S. Gupta, Atmos. Environ. 41 (2007) 4097–4105.

[22] Y.H. Yeom, J. Henao, M.J. Li, W.M.H. Sachtler, E. Weitz, J. Catal. 231 (2005) 181–193.

[23] N.W. Cant, I.O.Y. Liu, Catal. Today 63 (2000) 133–146.

[24] H. Hamada, Y. Kintaichi, M. Sasaki, T. Ito, M. Tabata, Appl. Catal. 70 (1991) L15–L20.

[25] M. Misono, Y. Hirao, C. Yokoyama, Catal. Today 38 (1997) 157–162.

[26] R. Matarrese, H.H. Ingelsten, M. Skoglundh, J. Catal. 258 (2008) 386–392.

[27] T. Nanba, A. Obuchi, Y. Sugiura, C. Kouno, J. Uchisawa, S. Kushiyama, J. Catal. 211 (2002) 53–63.

[28] H.H. Ingelsten, M. Skoglundh, Catal. Lett. 106 (2006) 15–19.

[29] Y. Yeom, M. Li, A. Savara, W.M.H. Sachtler, E. Weitz, Catal. Today 136 (2008) 55–63.